

# Decadal Change in the Correlation Pattern between the Tibetan Plateau Winter Snow and the East Asian Summer Precipitation during 1979–2011

DONG SI AND YIHUI DING

*National Climate Center and Laboratory for Climate Studies, China Meteorological Administration, Beijing, China*

(Manuscript received 7 August 2012, in final form 21 March 2013)

## ABSTRACT

Observational evidence indicates that the correlation between Tibetan Plateau (TP) winter snow and East Asian (EA) summer precipitation changed in the late 1990s. During the period 1979–99, the positive correlation between the TP winter snow and the summer precipitation along the Yangtze River valley (YRV) and southern Japan was disrupted by the decadal climate shift. In contrast, the summer precipitation over the Huaihe River valley (HRV) and the Korean Peninsula showed a strong positive correlation with the preceding winter snow over the TP during the period 2000–11.

The radiosonde temperature measurements over the TP show a pronounced warming since the late 1990s. This warming is associated with the significant increase in surface sensible heat flux and longwave radiation into atmosphere. The latter is closely related to the decrease of surface albedo and the soil hydrological effect of melting snow due to the decadal decrease in the preceding winter and spring snow over the TP. The TP warming induced by the decrease in winter snow, together with the cooling of the sea surface temperature in the tropical central and eastern Pacific, intensifies the land–sea thermal contrast in the subsequent spring and summer over EA, thus causing a northward advance of the EA summer monsoon. Accompanying the northward migration of the summer monsoon, the summer precipitation belt over EA shifts northward. Consequently, the high summer precipitation region over EA correlating with the preceding winter snow over the TP has shifted northward from the YRV and southern Japan to the HRV and the Korean Peninsula since the late 1990s.

## 1. Introduction

The Tibetan Plateau (TP), which has an average altitude of approximately 4 km, is one of the earth's most complex geographical features. The TP serves not only as a physical barrier but also as an elevated heat source that establishes a thermal contrast between the plateau and surrounding cooler air in the summer (Ding 1992). The combination of these two significant effects appears to be a central factor influencing the large-scale monsoon circulation over East Asia (EA) (e.g., Flohn 1957; Li and Yanai 1996). The seasonal cycle and interannual variation in the EA summer monsoon rainfall are known to be closely related to variations in TP heating (Ye and Gao 1979; Tao and Ding 1981; Hsu and Liu 2003; Wu and Qian 2003; Zhao et al. 2007). Zhang et al. (2004) and Ding et al. (2009) examined the relationship between

winter and spring snow cover over the TP and the decadal variations of the EA summer monsoon rainfall based on the observed data for the period from the 1960s to 1990s. Correlation analysis documented that the TP winter snow has a significant positive correlation with the subsequent summer precipitation along the Yangtze River valley (YRV; 28°–31°N, 110°–120°E) in China. It is proposed that an increase in the winter snow cover over the TP is closely related to a significant reduction in surface sensible heat flux and a subsequent cooling over the TP and its surrounding atmosphere. The cooling is caused by the surface albedo and soil hydrological effect of melting snow owing to the snow increase over the TP. TP cooling thus reduces the land–sea thermal contrast during summer over EA, leading to a weak EA summer monsoon, which brings more precipitation to the YRV (Ding et al. 2009).

Recently, Si et al. (2009) found that summer precipitation in EA exhibited a decadal shift in the late 1990s. During the 1980s and 1990s summer precipitation was mainly concentrated along the YRV. Since the late 1990s the precipitation belt has shifted northward to the

---

*Corresponding author address:* Dr. Dong Si, National Climate Center, China Meteorological Administration, No. 46 Zhong-guancun South Street, Haidian District, Beijing, 100081, China.  
E-mail: sidong@cma.gov.cn

Huaihe River valley (HRV;  $31^{\circ}$ – $33^{\circ}$ N,  $110^{\circ}$ – $120^{\circ}$ E), which has an average distance of 200–300 km from the YRV. However, the winter snow cover over the TP has shown a significant decreasing trend since the late 1990s. That is to say, both the TP winter snow and the EA summer precipitation have undergone a decadal change in the late 1990s, which naturally raises questions as to whether the TP snow–EA precipitation correlation pattern also experienced a similar change in the late 1990s and, if so, what new correlation pattern between the TP winter snow and the subsequent summer precipitation over EA has been established. With these questions in mind, we will examine the decadal change in the correlation between the TP winter snow and the EA summer precipitation in the last decade. Additionally, a physical mechanism responsible for the change in the TP snow–EA precipitation correlation in the last decadal period is discussed.

This paper is arranged as follows. Section 2 describes the datasets used in this study. In section 3, we document the decadal decreases in the winter and spring snow over the TP, while in section 4 we examine the decadal changes in summer precipitation over EA in the last decade. In section 5, we compare the correlation patterns of the winter snow cover over the TP with summer precipitation in EA between the two periods of 1979–99 and 2000–11. Plausible causes for these changes are discussed in section 6. A summary is provided in section 7.

## 2. Data

The main observational data analyzed in this study include the following products.

- 1) The daily surface-observed snow depth, wind speed, air temperature, soil temperature, and pressure data used in this study are from the National Meteorological Information Center (NMIC) of the China Meteorological Administration (CMA). The monthly data are derived from daily data. Because surface observing stations in the western TP begin providing operational observations since the late 1970s, our research is performed using data records starting from 1979 to add more observations in the western TP. In this study, 72 stations (Fig. 1) located where there is good temporal continuity in meteorological observations are used. The quality control of this dataset was made by the NMIC of the CMA.
- 2) Monthly station rainfall data include 160 stations in China, 11 stations in southern Japan, and 8 stations in South Korea. The Chinese station data are provided by the National Climate Center of the CMA included information from 160 stations, of which we chose 46 stations located in east China. Station data in southern

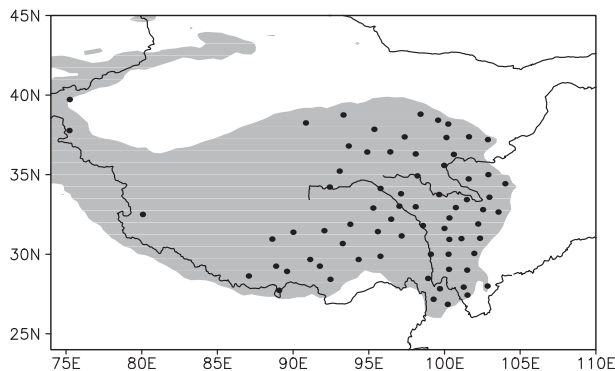


FIG. 1. Distribution of the 72 surface-observing stations (black dots) over the Tibetan Plateau. The shaded area (gray) indicates regions with an altitude above 2500 m.

- Japan and South Korea are derived from the Global Historical Climate Network (GHCN) of the National Climate Data Center (NCDC) of the National Oceanic and Atmospheric Administration (NOAA).
- 3) Radiosonde temperature data (Guo and Ding 2009) are provided by the NMIC of the CMA. Twice-daily observational data at 0000 and 1200 UTC are combined into a merged daily radiosonde temperature dataset. The quality control of this dataset also was done by the NMIC of the CMA recently.
  - 4) The National Aeronautics and Space Administration (NASA) Global Energy and Water Cycle Experiment (GEWEX) Surface Radiation Budget (SRB) release 3.1 dataset (Cox et al. 2006; Gupta et al. 2006) also is used in this study. This dataset uses International Satellite Cloud Climatology Project (ISCCP) clouds and radiance and other inputs to produce monthly mean upward and downward longwave radiative flux on a  $1^{\circ}$  latitude  $\times$   $1^{\circ}$  longitude resolution. The current release 3.1 covers the period from July 1983 through December 2007.
  - 5) The atmospheric data are derived from the National Centers for Environmental Prediction (NCEP)–National Center for Atmospheric Research (NCAR) reanalysis dataset (Kalnay et al. 1996).
  - 6) Monthly mean sea surface temperature (SST) data used are the optimum interpolated SST (OISST) dataset (Reynolds and Smith 1994) provided by NOAA at a  $2^{\circ}$  latitude  $\times$   $2^{\circ}$  longitude resolution.

## 3. Observed decreasing trend in the TP winter and spring snow

An examination of the observed snow depth data reveals that a prominent reduction in the winter and spring snow depth occurred throughout the TP during the last decade. Figure 2 depicts the time series of snow depths

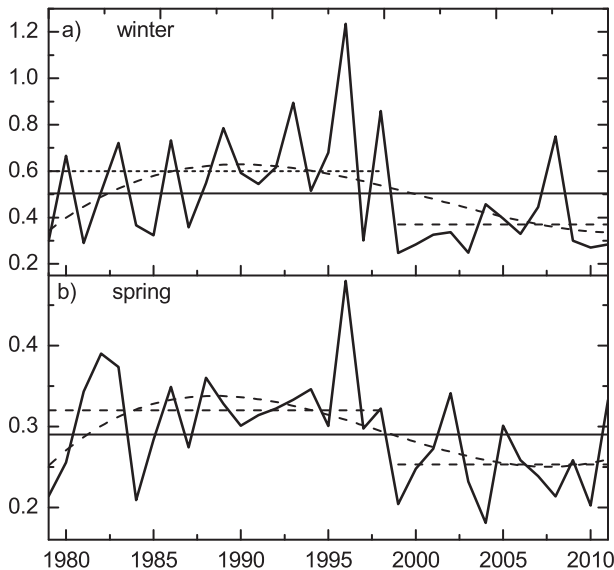


FIG. 2. Time series of (a) winter and (b) spring snow depth ( $\text{cm day}^{-1}$ ) over the Tibetan Plateau, averaged for the 72 stations from 1979 to 2011. The dashed curve indicates the third-order polynomial fit. The horizontal dashed lines indicate averaged values for the two decadal periods 1979–99 and 2000–11. The horizontal solid lines indicate averaged values for the period 1979–2011.

over the TP averaged for the 72 stations in winter and spring during the period 1979–2011. It can be seen that the winter and spring snow depth over the TP experienced a distinct decadal change in the late 1990s. This decadal change point is further confirmed by the Yamamoto method and Mann–Kendall method. The snow depth increases greatly from 1979 to 1996 and then decreases abruptly from 1996 to 1999. Since 1999 snow depth remains low except in winter 2008, possibly due to interannual variation. The average winter snow depth is  $0.6 \text{ cm day}^{-1}$  during 1979–99, but it drops to an average of  $0.37 \text{ cm day}^{-1}$  for the period 2000–11. The average spring snow depth is  $0.32 \text{ cm day}^{-1}$  during 1979–99, but it drops to an average of  $0.25 \text{ cm day}^{-1}$  for the period of 2000–11. Figure 3 presents the decadal change (2000–11 mean minus the 1979–99 mean, as below) in the winter snow depth over the TP. The regions experiencing significant snow reduction cover the majority of the TP.

#### 4. Summer precipitation changes in East Asia

In tandem with a reduction in winter and spring snow throughout the TP, the precipitation and large-scale atmospheric circulation in EA have experienced considerable changes. Recently, Si et al. (2009) found that the summer precipitation in east China exhibited a substantial decadal shift in the late 1990s. Before 1999, the main precipitation belt was located along the YRV; subsequently, it has steadily shifted northward to the HRV.

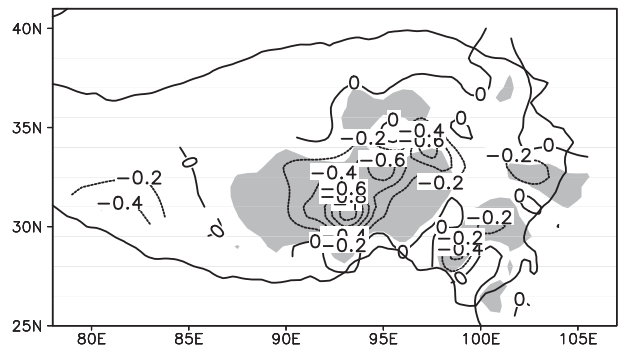


FIG. 3. Changes (2000–11 mean minus 1980–99 mean) in winter snow depth ( $\text{cm day}^{-1}$ ) over the Tibetan Plateau based on the surface-observed data. The shaded areas are statistically significant at the 95% confidence level according to a Student's *t* test.

Figure 4 displays the difference in summer precipitation patterns between 2000–11 and 1979–99 in east China. The most notable features are the two coherent zonal bands of precipitation anomalies, with opposite signs, over the YRV and HRV. One zonal area of negative anomalies is found along the YRV. Across the HRV, large precipitation anomalies with opposite signs are also observed. This pattern resembles the second leading mode of the empirical orthogonal function (EOF) analysis for the summer precipitation in east China in Si et al. (2009). Si et al. analyzed the spatial and temporal variation of the summer precipitation over the YRV and HRV and found that the second leading mode accounted for 21% of the total variance. This mode was characterized by a seesaw between the YRV and HRV (see Si et al. 2009, Fig. 1d). The time coefficients of the second leading mode also displayed an abrupt phase transition from negative to positive in the late 1990s (see Si et al. 2009, Fig. 1e). This change indicates that the summer precipitation has increased over the HRV but decreased over the YRV since the late 1990s.

Figure 5 shows the spatial pattern of contemporaneous correlation between the time series of summer precipitation averaged over the YRV/HRV and summer precipitation series of each of the 65 stations in EA. The most striking feature revealed by this figure is that the precipitation variations over southern Japan and Korean Peninsula are in phase with precipitation over YRV/HRV, showing a positive relationship. This correlation pattern also agrees with the results of Ninomiya and Akiyama (1992) and Ding and Chan (2005), who found that the mean summer precipitation belt over EA is normally elongated and narrow, extending from east China to southern Japan.

Therefore, the decadal change in the summer precipitation over east China in the late 1990s is not a local phenomenon but is connected to the shift in the large-scale

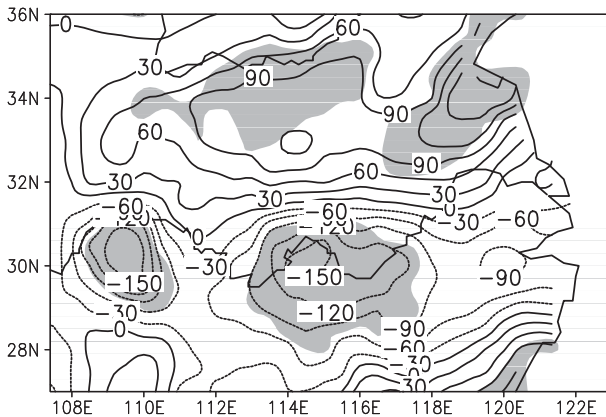


FIG. 4. Changes (2000–11 mean minus 1980–99 mean) in total summer precipitation (mm) over east China. The shaded areas are statistically significant at the 95% confidence level according to a Student's  $t$  test.

precipitation regime over EA. For southern Japan, the precipitation is also relatively high during the 1980s and 1990s, but relatively low during the 2000s. In contrast, the summer precipitation levels on Korean Peninsula are relatively low during the 1980s and 1990s but are comparatively high during the 2000s (not shown). This trend implies that the primary summer precipitation belt, indeed, shifted northward throughout EA in the late 1990s.

The changes in summer precipitation patterns throughout EA are revealed by EOF analysis. The normalized observed summer [June–August (JJA)] precipitation in EA is used in the EOF analysis. The first EOF mode, which accounts for 16.6% of the total variance, displays a pattern of an elongated band of positive precipitation anomalies along the YRV, southern Japan, and southern South Korea and negative precipitation anomalies over other EA regions (Fig. 6a). The first EOF mode clearly indicates that the main precipitation belt extends from the YRV to southern Japan, and its time coefficient show a declining trend (Fig. 6b). The second EOF mode accounts for 14.2% of the total variance. The spatial pattern corresponds to coherent variations over HRV and the Korean Peninsula and opposite variations in YRV and the area south of YRV (Fig. 6c). Figure 6d illustrates the time coefficient of the second EOF mode, which shows an abrupt decadal change in the late 1990s. Moreover, the period from the early 1980s to 1990s is mainly in the negative phase of time coefficient, implying that it is wet in the YRV, the area south of YRV, and southern Japan but dry over the HRV and Korean Peninsula. Since the late 1990s the phase abruptly turns positive. This change implies the decadal northward shift of the precipitation belt. For the earlier decade (1979–99), the average value of absolute time coefficient of the first EOF mode is 2.51,

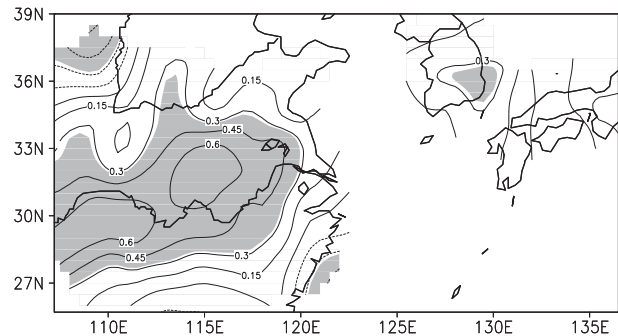


FIG. 5. Correlation map between the summer precipitation over the Yangtze River and Huaihe River valleys averaged for the 46 stations and summertime precipitation over East Asia for 1979–2011. The shaded areas are statistically significant at the 95% confidence level.

while the average value of absolute time coefficient of the second EOF mode is 2.26. This result indicates that the YRV–southern Japan mode is the leading mode during 1979 to 1999. For the later decade (2000–11), the average value of absolute time coefficient of the first EOF mode is 2.09, while the average value of the second EOF mode is 2.82. The first leading EA summer precipitation mode distinctly changes from a YRV–southern Japan mode during 1979–99 to an HRV–Korean Peninsula mode in the last decade (2000–11), indicating a decadal northward shift in the summer precipitation belt in EA.

All of these results reveal that the summer precipitation patterns in East China and EA have both demonstrated a decadal change in the late 1990s. This decadal change is opposite to the previous one in the late 1970s. The decadal change in precipitation over EA occurred in the late 1970s with more precipitation in the YRV and southern Japan and less in the HRV and the Korean Peninsula since then (e.g., Hu 1997; Chang et al. 2000; Huang 2001; Wang 2001; Gong and Ho. 2002; Yu et al. 2004; Ding et al. 2009; Zhou et al. 2009).

### 5. Decadal change in the TP snow–EA precipitation correlation

The above analysis reveals that both TP winter snow and the ensuing EA summer precipitation underwent a dramatic decadal change in the late 1990s. In this section, we will examine whether the correlation between TP winter snow and the following summer precipitation in EA changed in the late 1990s.

To elaborate on the relationship between the above two elements for the time periods of 1979–99 and 2000–11, a correlation analysis is applied to the winter snow depth over the TP and the following summer precipitation in EA.

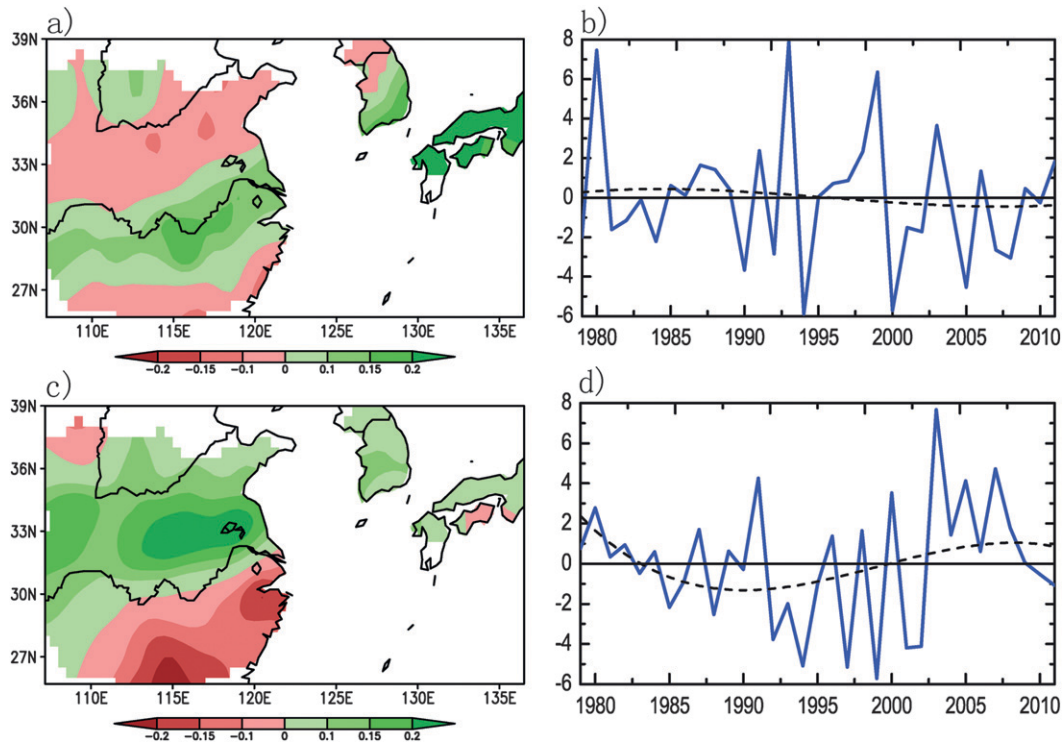


FIG. 6. Spatial pattern of (a) EOF1 and (c) EOF2 for summer precipitation and (b),(d) their corresponding time coefficient during 1979–2011. The dashed curves in (b),(d) indicate a third-order polynomial fit.

For the period 1979–99, the correlation map between the TP winter snow series (Fig. 2) and the summer rainfall in EA indicate a significant positive zonal band along the YRV and southern Japan (Fig. 7a). The correlation pattern obtained from the analysis implies that an above normal TP winter snow will be followed by increased precipitation along the YRV and southern Japan during the subsequent summer and vice versa.

However, for the period 2000–11 the correlation pattern changes radically and differs from the first period's pattern. The positive correlation shift northward from the YRV and southern Japan to the HRV and the Korean Peninsula, while a negative correlation along the YRV and southern Japan is detected (Fig. 7b). The result suggests that an above normal TP winter snow favors increased summer precipitation along the YHR–Korean Peninsula and decreased summer precipitation along YRV–southern Japan. This change implies a decadal change in the correlation pattern between the TP snow and the EA summer precipitation in the late 1990s.

## 6. Causes of the decadal change in the TP snow–EA precipitation correlation

We present a brief description in this section of why the regions of high correlation between the TP winter

snow and the subsequent summer precipitation over East Asia have shifted northward from the YRV to the HRV. This may be closely related to the decadal reduction in the snow over the TP since the late 1990s. It is known that an anomalous preceding winter snow cover may affect the surface albedo and influence soil hydrology, which may further alter the soil moisture and surface and atmosphere temperature during the subsequent summer, thus leading to variations in the ensuing large-scale atmospheric circulation and the Asian summer monsoon (Liu and Yanai, 2002). Shukla (1984) and Shukla and Mooley (1987) pointed out that the memory of a winter snow anomaly in the climate system resides in the wetness of the subsurface soil as snow melts during spring and summer, which influences the soil and air temperature in the following summer and affects the regional monsoon circulation. Figure 8a illustrates the lagging effect of winter snow depth on the summer thermal condition over the TP by using a lead–lag correlation. We denote the high snow depth as year 0 and the following year as year 1. For the winter snow depth over the TP, the high snow depth peaks during January–February (1) and persists to early spring. Snow melting (Fig. 8a, red curve) begins to develop a significantly positive correlation with snow depth in March (1), which persists to April (1). Snow melting is a sink for latent heat;

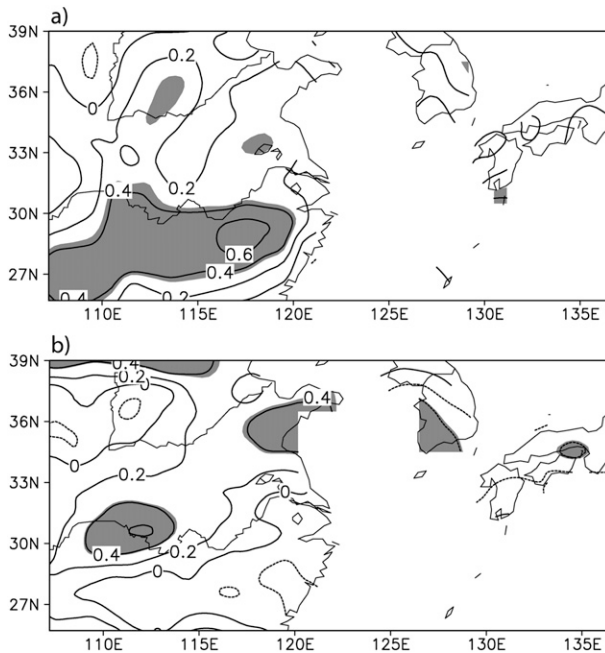


FIG. 7. Correlation between the winter snow depth over the Tibetan Plateau averaged for the 72 stations and the observed summer precipitation over East Asia for the period (a) 1979–99 and (b) 2000–11. Shaded areas are statistically significant at the 95% confidence level.

snow melts to water that is available for evaporation, runoff, and to increase soil moisture by diffusion and gravitational transport (Vernekar et al. 1995). The top layer (0–7 cm) soil moisture (Fig. 8a, green curve) anomalies have a moderate persistence from winter to mid spring. High persistence is seen in the middle layer (28–100 cm) soil moisture (Fig. 8a, blue curve) and persists to late spring. This result is consistent with a longer persistence of soil moisture for the middle layer than the top layer in an earlier analysis of a numerical simulation by Wang et al. (2009). A significantly negative correlation with soil temperature (Fig. 8b, red curve), sensible heat flux (Fig. 8b, green curve), and air temperature (Fig. 8b, blue curve) persists from December (0) to March (1). This is largely because of the snow albedo effect. When snow is present on the ground, the soil and air temperature is colder than without snow. After March (1), a large amount of snow melts and effectively decreases the snowpack and the albedo effect. Snowmelt water increases not only the soil moisture but also the heat capacity of the soil. The air temperature retains a high negative correlation long after all of the snow is melted because of the large heat capacity of the wetter surface. However, air temperature is not significantly correlated with the winter snow depth in May (1) when most of the snow over the TP has melted. In summary, the air

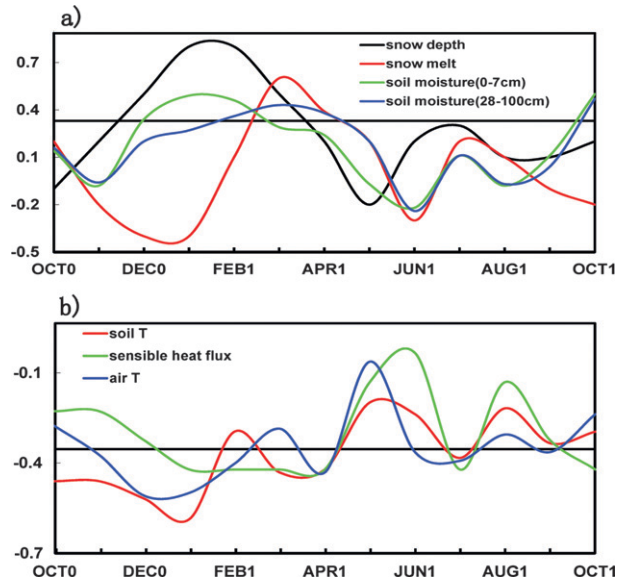


FIG. 8. (a) Correlation of the TP snow depth with the TP snowmelt (change of monthly snow depth, red curve), 0–7-cm-deep volumetric soil moisture (green curve), and 28–100-cm-deep volumetric soil moisture (blue curve) of the ECMWF Interim Re-Analysis for December (0)–February (1) at the 72 stations (29°–35°N, 90°–104°E) for the period 1979–2011. Note that the high snow-depth year designated as year 0 and following year as year 1. The black solid curve is for the autocorrelation of the TP snow depth with its December–February (DJF) values. (b) Correlation of the TP snow depth with the TP soil temperature (red curve), sensible heat flux (green curve), and air temperature (blue curve) for December (0)–February (1) at the 72 stations for the period 1979–2011.

temperature over the TP is low because of the snow albedo effect in winter, heat loss energy used in melting snowpack, and the larger heat capacity of the wetter soil from spring and summer.

The anomalous snow condition over the TP may significantly affect the TP heating field. Based on previous estimates of heat sources and sinks over the TP in summer, the surface sensible heat flux is a dominant component of atmospheric heating field over the TP, especially over the western part of the TP (Ye and Gao 1979; Nitta 1981; Murakami and Ding 1982; Luo and Yanai 1984). Ye and Gao (1979) computed various components of long-term mean heat balanced over the TP and their seasonal variations, and pointed out that the sensible heating is the primary factor in atmospheric heating sources over the entire TP until the rainy season occurs.

We have estimated sensible heat flux by using the 72 station observed data. The sensible heat ( $H$ ) is calculated by

$$H = \rho c_p C_H U (T_s - T_a), \quad (1)$$

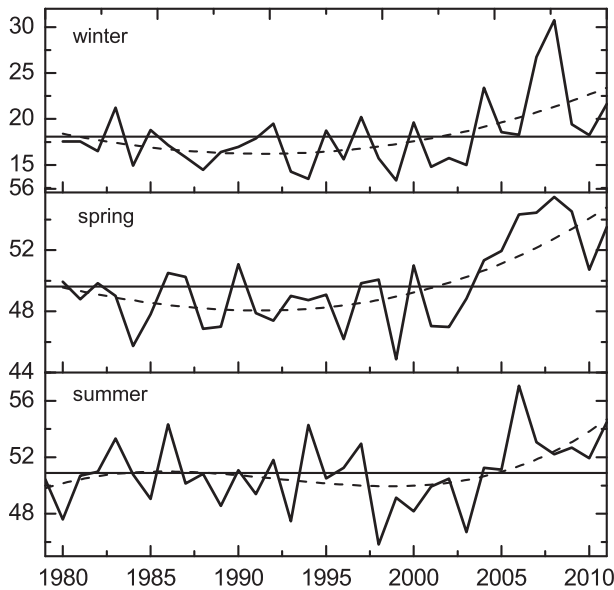


FIG. 9. Seasonal-mean sensible heat fluxes ( $\text{W m}^{-2}$ ) over the TP averaged for the 72 stations for (a) winter, (b) spring, and (c) summer. The dashed curve indicates a third-order polynomial fit; horizontal solid lines indicate averaged values for the period of 1979–2011.

where  $\rho$  is air density,  $C_p$  the specific heat at a constant pressure,  $U$  the wind speed,  $T_s$  the soil temperature,  $T_a$  is near-surface air temperature, and

$$C_H = 0.0012 + 0.01/U \quad (2)$$

(Chen and Wong 1984).

Figure 9 shows the seasonal mean sensible heat fluxes over the TP averaged for the 72 station during the period 1979–2011. Significant increasing trends in sensible heat flux, derived by using a third-order polynomial fit, are obvious in all three seasons since the late 1990s. The trend in summer is  $0.6\% \text{ decade}^{-1}$ . It is in winter when the trend is most notable,  $1.6\% \text{ decade}^{-1}$ . The trend in spring is comparably strong,  $1.5\% \text{ decade}^{-1}$ .

Additionally, TP warming is an important factor driving the Asian summer monsoon. The seasonal variation in TP heating is closely associated with the anomalous reversal of the zonal thermal contrast in the Asian monsoon region. This variation, therefore, may influence the large-scale atmospheric circulation and summer monsoon in EA (Flohn 1957; Yanai et al. 1992; Li and Yanai 1996; Wu and Zhang 1998; Wang et al. 2008). Figure 10 shows the decadal changes in surface longwave radiation ratio (surface longwave upward flux/downward flux) over the TP. For winter, the decadal difference in surface longwave radiation ratio is positive over the entire plateau; that is, it represents the TP warming over most of

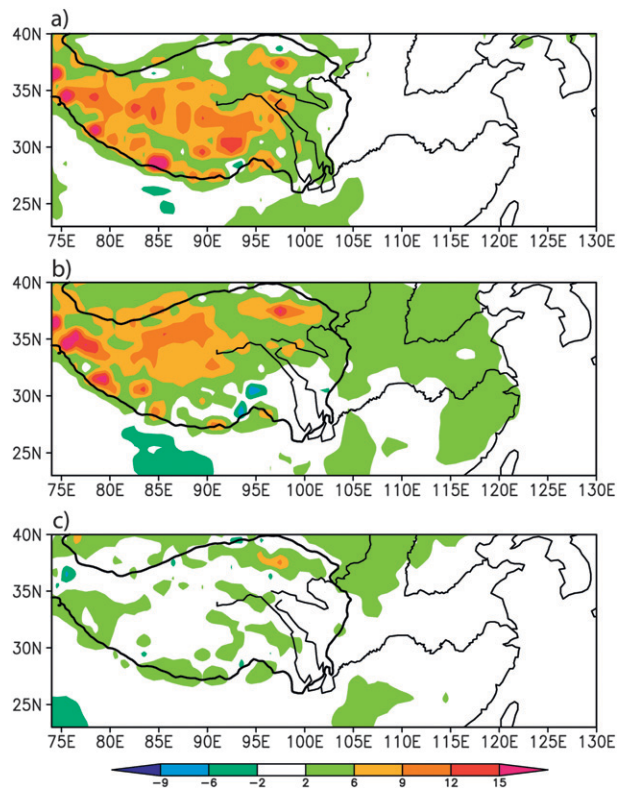


FIG. 10. Changes (2000–07 mean minus 1984–99 mean) in the surface longwave radiation ratio (%) (upward flux/downward flux) in (a) winter, (b) spring, and (c) summer.

the TP in the later decade, with surface longwave radiation ratio increasing by 2%–9%—even by 9%–15% in a few regions. A similar difference between the two periods, but with a relative smaller warming tendency, also appears in spring and summer.

We also examine the temperature series mostly in the central and eastern TP averaged for the 15 stations (Fig. 11a) at five levels from 1979 to 2011 (Figs. 11b,c). A remarkable feature is that the radiosonde temperature exhibits a prominent decadal change in the late 1990s. A distinctive tropospheric (from 500 to 200 hPa) warming trend and stratospheric (100 hPa) cooling trend are found over the TP in spring. The warming trend is most prominent in the upper troposphere and around 300 hPa. For summer, warming also occurs in the troposphere, with the amplitude of the warming tending to strengthen with increasing altitude, shifting to a cooling trend above 200 hPa. The tropospheric warming trend over the TP is notably more pronounced in summer than in spring.

Augmented atmospheric warming in the spring and summer over the TP since the late 1990s may, in turn, influence the land–sea thermal contrast in the EA monsoon region. Previous research revealed a positive correlation between TP snow and oceanic forcing (SST

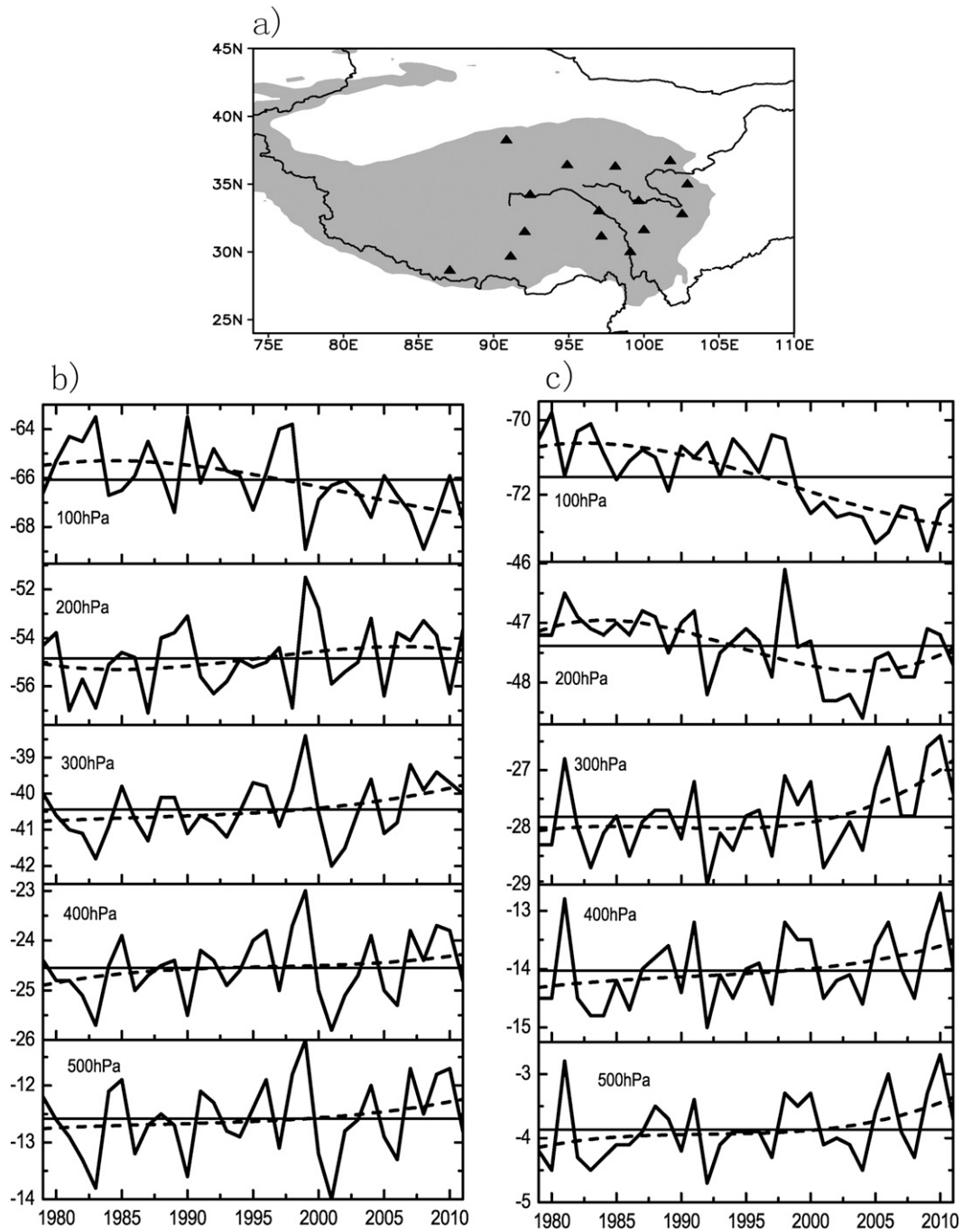


FIG. 11. (a) Distribution of the 15 radiosonde stations over the Tibetan Plateau and (b) spring and (c) summer temperature (°C) over the TP averaged for the 15 stations from 500 to 100 hPa. The horizontal solid lines indicate averaged values for the period of 1999–2011; Dashed curves indicate a third-order polynomial fits.

anomalies in the tropical central and eastern Pacific), and both factors had a high negative correlation with the land–sea thermal contrast in the EA monsoon region (Ding et al. 2009). This result implies that, if the TP has below normal (above normal) snow in the preceding winter and the tropical central and eastern Pacific

anomalously cools down (warms up), the land–sea thermal contrast in the EA monsoon region will intensify during the subsequent spring and summer. Based on the computational methods discussed by Yanai et al. (1992), the vertically integrated (surface to 200 hPa) apparent heat source  $Q_1$  is estimated by using the NCEP–NCAR

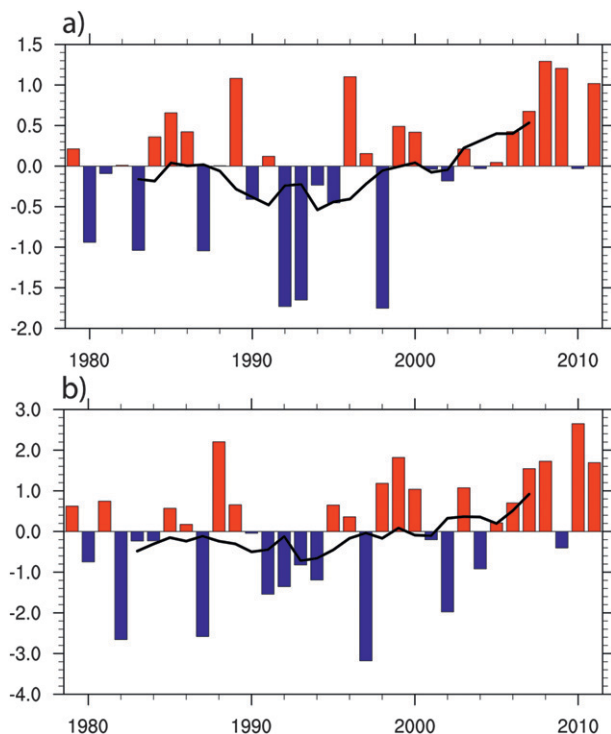


FIG. 12. Time series of the difference between the normalized vertically integrated (from surface to 200 hPa) apparent heat source  $Q_1$  ( $\text{W m}^{-2}$ ) averaged over the Tibetan Plateau ( $28^{\circ}$ – $43^{\circ}\text{N}$ ,  $70^{\circ}$ – $105^{\circ}\text{E}$ ) and the tropical central and eastern Pacific ( $10^{\circ}\text{S}$ – $10^{\circ}\text{N}$ ,  $180^{\circ}$ – $120^{\circ}\text{W}$ ) for (a) spring and (b) summer. The solid lines denote 9-yr running mean curves.

reanalysis dataset. Here, the difference of  $Q_1$  between the TP and the tropical central and eastern Pacific is defined as the land–sea thermal contrast index. The higher the thermal contrast index, the more amplified the land–sea thermal contrast. The time series of the land–sea thermal contrast index for 1979–2011 is depicted in Fig. 12, which shows a distinct rising trend and a change in sign from negative to positive since the late 1990s, indicating an augmented land–sea thermal contrast in the EA monsoon region.

As the land–sea thermal contrast increases, the large-scale atmospheric circulation changes over the EA monsoon region during the subsequent spring and summer. Under the above forcing of the heightened land–sea thermal contrast, the northern boundary of the EA summer monsoon migrates northward. As seen from Fig. 13, anomalous low-level westerly winds decrease along the YRV, and anomalous westerly winds simultaneously increase along the HRV, indicating the northward migration of the northern boundary of the summer monsoon over EA. The anomalous cyclonic circulation strengthens over the HRV while it weakens over the YRV. Thus, the precipitation belt is located along the HRV but departs

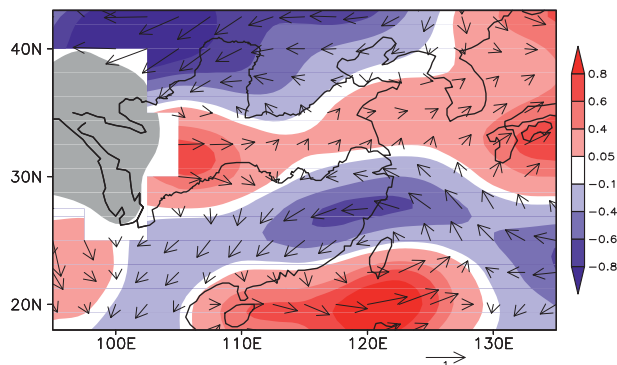


FIG. 13. Changes (2000–11 mean minus 1980–99 mean) in 850-hPa zonal components (red shading denotes westerly components and blue shading denotes easterly components,  $\text{m s}^{-1}$ ) and 850-hPa winds (vectors,  $\text{m s}^{-1}$ ) in summer. The shaded area (gray) indicates altitudes above 2500 m.

from the YRV (Fig. 4). Accompanying the northward advance of the summer monsoon, the EA monsoon subsystems also shift northward.

Because the westerly subtropical jet marks the poleward limit of the Hadley cell, a systematic northward shift of the jet implies that the Hadley cell expands northward in the Northern Hemisphere. Figure 14a illustrates the change in outgoing longwave radiation (OLR) in the summer. Enhanced convection is obtained in the climatological tropical western North Pacific intertropical convergence zone (ITCZ) and areas to its north, where the climatological OLR values are less than  $220 \text{ W m}^{-2}$  along  $0^{\circ}$ – $13^{\circ}\text{N}$ , implying that the tropical western Pacific ITCZ is enhanced and displaced northward. However, convection is suppressed to the north of the climatological western North Pacific subtropical high (WNPSH) where the climatological OLR values are greater than  $250 \text{ W m}^{-2}$  along  $20^{\circ}$ – $30^{\circ}\text{N}$ , implying that the WNPSH is enhanced and displaced northward as well. The change in the WNPSH is more evident in the 500-hPa geopotential height difference for the 2000–11 mean minus 1980–99 mean. As seen from Fig. 14b, geopotential height is raised in an extensive area to the north of the climatological WNPSH, where the climatological 500-hPa geopotential height values are greater than 5880 gpm, whereas it drops in the extensive area to the south of the climatological WNPSH, further verifying the northward displacement of the WNPSH. Because the locations of the ITCZ and WNPSH are considered as rising and subsiding branches of the Hadley cell, respectively, an enhancement and northward displacement of the ITCZ and the WNPSH implies that the local Hadley cell in EA intensified and expanded northward during the last decade. Because subsidence causes adiabatic heating and suppresses convection, this northward expansion leads to midlatitude (near  $30^{\circ}\text{N}$ ) tropospheric warming

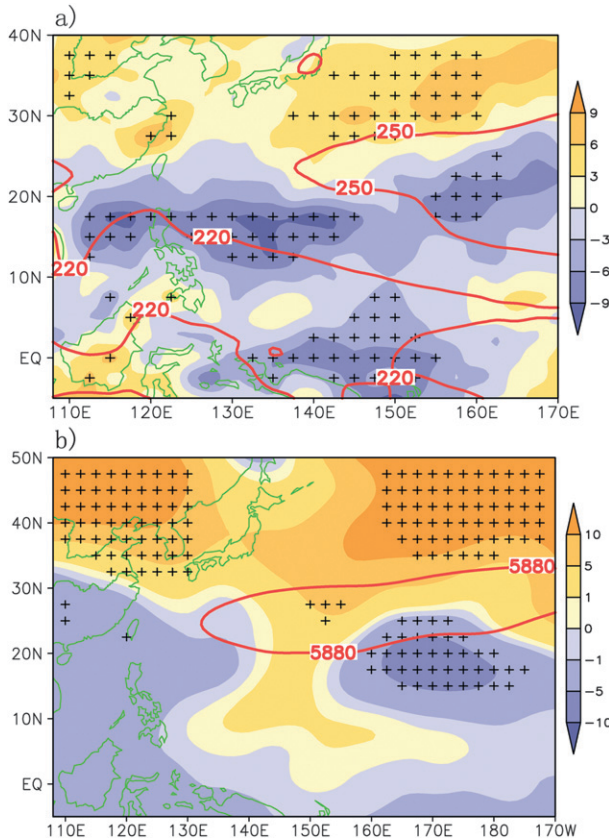


FIG. 14. (a) Changes (2000–11 mean minus 1980–99 mean) in outgoing longwave radiation ( $\text{W m}^{-2}$ ) in summer. The red thick contours indicate the climatological outgoing longwave radiation distribution averaged for summer in 1981–2010. Values exceeding the 95% confidence level according to a Student's  $t$  test are stippled. (b) Changes (2000–11 mean minus 1980–99 mean) in 500-hPa geopotential height (gpm) in summer. The red thick contours indicate the climatological 500-hPa geopotential height distribution averaged for summer in 1981–2010. Values exceeding the 95% confidence level according to a Student's  $t$  test are stippled.

and a broadening of subtropical dry zones (near  $30^{\circ}\text{N}$ ) (Fu et al. 2006; Hu and Fu 2007), which would contribute to a decrease in summer precipitation along the YRV and southern Japan, but an increase summer precipitation along the HRV and Korean Peninsula.

As previously noted, water vapor transport is one of the most important components of the EA monsoon system. Anomalous precipitation is directly related to water vapor transport. Here, an analysis is made to examine the differences in water vapor transport over the EA monsoon region between the periods 1979–99 and 2000–11.

Figure 15 displays the anomalous composite field of the 850-hPa water vapor transport for 1979–99 and 2000–11. The shaded areas indicate the convergence of the anomalous water vapor. During 1979–99 the tropical

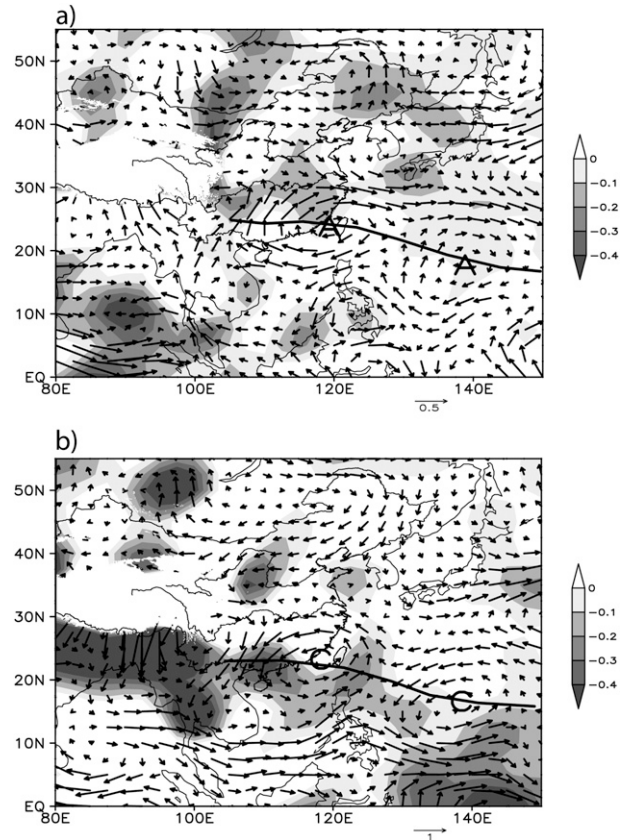


FIG. 15. Anomalous 850-hPa water vapor transport ( $\text{kg m}^{-1} \text{s}^{-1}$ ) in summer for the period (a) 1979–99 and (b) 2000–11. The divergence of water vapor transports is plotted in shading; A (C) mark the centers of the anomalous anticyclone (cyclone); the dashed curves indicate the anomalous anticyclone (cyclone) ridge (trough).

southwest water vapor transport converges with the northwest midlatitude water vapor transport above the main rain belt along the YRV and southern Japan. This anomalous water vapor transport is associated with a southward displacement of the WNPSH and a southward migration of the northern boundary of the EA summer monsoon. During 2000–11, in contrast, the water vapor convergence zone moves northward to the HRV and Korean Peninsula. The origin of the anomalous convergence is from the subtropical southeast water vapor transport and the northeast midlatitude water vapor transport. The subtropical southeast branch originates from the East China Sea. This anomalous water vapor transport is associated with a northward displacement of the WNPSH and a northward migration of the northern boundary of the EA summer monsoon, which is favorable for a heavier rain belt along the HRV (Zhou and Yu, 2005) and Korean Peninsula.

Another phenomenon in the anomalous water vapor transport pattern worth discussion is the ENSO signal

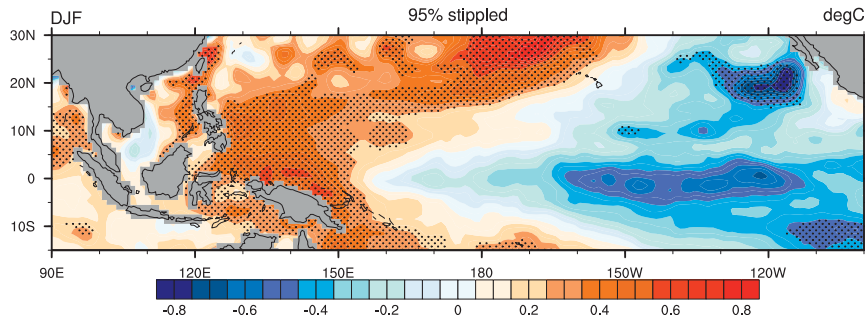


FIG. 16. Changes (2000–11 mean minus 1982–99 mean) in observed winter sea surface temperature ( $^{\circ}\text{C}$ ) based on the NOAA OISST data. Values exceeding the 95% confidence level according to a Student's  $t$  test are stippled.

from the tropical central and eastern Pacific. Throughout the period 1979–99, the circulation anomalies at low latitudes are dominated by an elongated anticyclonic ridge extending from the southeast coast of China to the western Pacific. This ridge has two centers at  $22^{\circ}\text{N}$ ,  $120^{\circ}\text{E}$  and  $20^{\circ}\text{N}$ ,  $140^{\circ}\text{E}$ . This anomalous anticyclonic ridge conveys, in part, the impacts of warm tropical central and eastern Pacific SSTs to the EA climate through the Pacific–East Asia teleconnection (Wang et al. 2000; Wang and Zhang 2002), which leads to a higher water vapor supply to the YRV and southern Japan. During the later period of 2000–11, the anomalous circulation change occurs at the low latitudes of EA and the former anticyclonic ridge is replaced by a cyclonic trough. This decadal shift results from the decadal change in the remote forcing produced by the tropical central and eastern Pacific SST anomaly. During the 1980s and 1990s, the SST over the tropical central and eastern Pacific is relatively high. Since the late 1990s, the central and eastern Pacific experiences a high La Niña event period, leading to a corresponding cold SST over the tropical central and eastern Pacific during the 2000s (Fig. 16).

Overall, the northward migration of the northern boundary of the summer monsoon, the subtropical westerly jet, the WNPSH and the local Hadley cell over EA results in the northward shift of the summer precipitation belt from the YRV and southern Japan to the HRV and Korean Peninsula. These results suggest that the connection between the northward shifts in the high summer precipitation throughout EA with the TP winter snow may be closely related to the significant decadal reduction in snow depth over the TP since the late 1990s.

## 7. Summary

A significant trend in the decline of winter and spring snow over the TP since the late 1990s is confirmed based on weather station observational data. This trend may exert some considerable influence on the precipitation

and large-scale atmospheric circulation over the TP and its surrounding areas, including the displacement of the primary summer precipitation belt and the northern boundary of the summer monsoon over EA. It is verified that the summer precipitation belt over EA experienced a decadal shift in the late 1990s. There is a remarkable difference between the periods prior to and following the late 1990s, with the summer precipitation belt chiefly located along the YRV and southern Japan before the late 1990s, subsequently shifting northward to the HRV and Korean Peninsula.

In addition, the correlation between the TP winter snow and the following summer precipitation in EA changed in the late 1990s. For the period from the 1980s to the 1990s, the correlation analysis reveals a strong positive correlation between the TP winter snow and the subsequent summer precipitation along the YRV and southern Japan. Since the late 1990s, however, the areas of strong positive correlation between the TP winter snow and summer precipitation over EA shift northward from the YRV and southern Japan to the HRV and Korean Peninsula, thus leading to a negative correlation along the YRV and southern Japan. An above normal winter TP snow favors increased precipitation along the HRV and the Korean Peninsula but decreased precipitation along the YRV and southern Japan in the subsequent summer.

Further analysis suggests that this change in correlation patterns is closely associated with the decadal decrease in snow over the TP since the late 1990s. The increase in TP heating, mainly owing to the decrease in winter snow, together with the decrease in SST in the tropical central and eastern Pacific, possibly enhances the land–sea thermal contrast over EA in the subsequent spring and summer. Thus, the northern boundary of the EA summer monsoon and the summer precipitation belt migrate northward. Correspondingly, the WNPSH and the local Hadley cell advance northward over East Asia, and the water vapor convergence zone moves northward from

the YRV and southern Japan to the HRV and Korean Peninsula. These changes led to an increase in precipitation over the HRV and Korean Peninsula and a decrease over the YRV and southern Japan in the subsequent summer. Thus, the decadal northward shift of the high correlation region over EA between the TP snow depth and the monsoonal precipitation in the late 1990s is closely related to the decrease in winter and spring snow over the TP. However, it is not apparent why the TP winter and spring snow has experienced a decadal-scale decrease.

For a long time period, the TP role, especially on the interannual time scale, in regional climate change is still an open question whether it plays an active role. This work provides evidence indicating the close relationship between decadal variations of the TP snow and that of the rainfall pattern in EA, but it does not mean logically that the rainfall anomaly pattern in EA is dominated completely by the TP snow variations as this relationship may be an indicator of, and is probably affected by, the external large-scale forcing from the interdecadal variation of SST in the Indian, Pacific, and even Atlantic Oceans, as well as polar ice concentration.

*Acknowledgments.* This work is jointly supported by the National Basic Research Program of China (2010CB950404, 2012CB955203, and 2013CB430202), the National Natural Science Foundation of China (41130960), and the CMA Special Public Welfare Research Fund (GYHY201006009). We thank the three anonymous reviewers and the editor for providing very useful critical comments on the paper.

## REFERENCES

- Chang, C.-P., Y. Zhang, and T. Li, 2000: Interannual and interdecadal variations of the East Asian summer monsoon and tropical Pacific SSTs. Part I: Roles of the subtropical ridge. *J. Climate*, **13**, 4310–4325.
- Chen, W., and D. Wong, 1984: A preliminary study on the computational method of 10-day mean sensible heat and latent heat on the Tibetan Plateau. *Collected Works of the Qinghai-Xizang Plateau Meteorological Experiment* (in Chinese), Vol. 2, Science Press, 35–45.
- Cox, S. J., P. W. Stackhouse, S. K. Gupta, J. C. Mikovitz, T. Zhang, L. M. Hinkelman, M. Wild, and A. Ohmura 2006: The NASA/GEWEX Surface Radiation Budget project: Overview and analysis. *Extended Abstracts, 12th Conf. on Atmospheric Radiation*, Madison, WI, Amer. Meteor. Soc., 10.1. [Available online at <https://ams.confex.com/ams/pdfpapers/112990.pdf>.]
- Ding, Y., 1992: Effects of the Qinghai–Xizang (Tibetan) Plateau on the circulation features over the plateau and its surrounding areas. *Adv. Atmos. Sci.*, **9**, 113–130.
- , and J. C. L. Chan, 2005: The East Asian summer monsoon: An overview. *Meteor. Atmos. Phys.*, **89**, 117–142.
- , Y. Sun, Z. Wang, Y. Zhu, and Y. Song, 2009: Inter-decadal variation of the summer precipitation in China and its association with decreasing Asian summer monsoon. Part II: Possible causes. *Int. J. Climatol.*, **29**, 1926–1944, doi:10.1002/joc.1759.
- Flohn, H., 1957: Large-scale aspects of the summer monsoon in South and East Asia. *J. Meteor. Soc. Japan*, **75**, 180–186.
- Fu, Q., C. M. Johanson, J. M. Wallace, and T. Reichler, 2006: Enhanced mid-latitude tropospheric warming in satellite measurements. *Science*, **312**, 1179, doi:10.1126/science.1125566.
- Gong, D.-Y., and C.-H. Ho, 2002: Shift in the summer rainfall over the Yangtze River valley in the late 1970s. *Geophys. Res. Lett.*, **29** (10), doi:10.1029/2001GL014523.
- Guo, Y., and Y. Ding, 2009: Long-term free-atmosphere temperature trends in China derived from homogenized in situ radiosonde temperature series. *J. Climate*, **22**, 1037–1051.
- Gupta, S. K., P. W. Stackhouse, S. J. Cox, J. C. Mikovitz, and T. Zhang, 2006: Surface Radiation Budget Project completes 22-year data set. *GEWEX News*, Vol. 16, No. 4, International GEWEX Project Office, Silver Spring, MD, 12–13.
- Hsu, H.-H., and X. Liu, 2003: Relationship between the Tibetan Plateau heating and East Asian summer monsoon rainfall. *Geophys. Res. Lett.*, **30**, 2066, doi:10.1029/2003GL017909.
- Hu, Y., and Q. Fu, 2007: Observed poleward expansion of the Hadley circulation since 1979. *Atmos. Chem. Phys.*, **7**, 5229–5236.
- Hu, Z.-Z., 1997: Interdecadal variability of summer climate over East Asia and its association with 500 hPa height and global sea surface temperature. *J. Geophys. Res.*, **102**, 19 403–19 412.
- Huang, R., 2001: Decadal variability of the summer monsoon rainfall in East Asia and its association with the SST anomalies in the tropical Pacific. CLIVAR Exchanges, No. 6, International CLIVAR Project Office, Southampton, United Kingdom, 7–8.
- Kalnay, E., and Coauthors, 1996: The NCEP/NCAR 40-Year Reanalysis Project. *Bull. Amer. Meteor. Soc.*, **77**, 437–471.
- Li, C., and M. Yanai, 1996: The onset and interannual variability of the Asian summer monsoon in relation to land–sea thermal contrast. *J. Climate*, **9**, 358–375.
- Liu, X., and M. Yanai, 2002: Influence of Eurasian spring snow cover on Asian summer rainfall. *Int. J. Climatol.*, **22**, 1075–1089.
- Luo, H., and M. Yanai, 1984: The large-scale circulation and heat sources over the Tibetan Plateau and surrounding areas during the early summer of 1979. Part II: Heat and moisture budgets. *Mon. Wea. Rev.*, **112**, 966–989.
- Murakami, T., and Y. Ding, 1982: Wind and temperature changes over Eurasia during the early summer of 1979. *J. Meteor. Soc. Japan*, **60**, 183–196.
- Ninomiya, K., and T. Akiyama, 1992: Multi-scale features of Baiu, the summer monsoon over Japan and the East Asia. *J. Meteor. Soc. Japan*, **70**, 467–495.
- Nitta, T., 1981: Observational study of heat sources over the eastern Tibetan Plateau during the summer monsoon. *J. Meteor. Soc. Japan*, **59**, 590–605.
- Reynolds, R. W., and T. M. Smith, 1994: Improved global sea surface temperature analyses using optimum interpolation. *J. Climate*, **7**, 929–948.
- Shukla, J., 1984: Predictability of time averages. Part II: The influence of the boundary forcing. *Problems and Prospects in Long and Medium Range Weather Forecasting*, D. M. Burridge and E. Kallen, Eds., Springer-Verlag, 155–206.
- , and D. A. Mooley, 1987: Empirical prediction of the summer monsoon rainfall over India. *Mon. Wea. Rev.*, **115**, 695–704.
- Si, D., Y. Ding, and Y. Liu, 2009: Decadal northward shift of the Meiyu belt and the possible cause. *Chin. Sci. Bull.*, **54**, 4742–4748.

- Tao, S., and Y. Ding, 1981: Observational evidence of the influence of the Qinghai–Xizang (Tibet) Plateau on the occurrence of heavy rain and severe convective storms in China. *Bull. Amer. Meteor. Soc.*, **62**, 23–30.
- Vernekar, A. D., J. Zhou, and J. Shukla, 1995: The effect of Eurasian snow cover on the Indian monsoon. *J. Climate*, **8**, 248–266.
- Wang, B., and Q. Zhang, 2002: Pacific–East Asian teleconnection. Part II: How the Philippine Sea anomalous anticyclone is established during El Niño development. *J. Climate*, **15**, 3252–3265.
- , R. Wu, and X. Fu, 2000: Pacific–East Asian teleconnection: How does ENSO affect East Asian climate? *J. Climate*, **13**, 1517–1536.
- , Q. Bao, B. Hoskins, G. Wu, and Y. Liu, 2008: Tibetan Plateau warming and precipitation changes in East Asia. *Geophys. Res. Lett.*, **35**, L14702, doi:10.1029/2008GL034330.
- Wang, H., 2001: The weakening of the Asian monsoon circulation after the end of 1970s. *Adv. Atmos. Sci.*, **18**, 376–386.
- Wang, R., W. Li, X. Liu, and L. Wang, 2009: Simulation of the impact of spring soil moisture over the Tibetan Plateau on summer precipitation in China (in Chinese). *Plateau Meteor.*, **28**, 1233–1241.
- Wu, G., and Y. Zhang, 1998: Tibetan Plateau forcing and the timing of the monsoon onset over South Asia and the South China Sea. *Mon. Wea. Rev.*, **126**, 913–927.
- Wu, T., and Z. Qian, 2003: The relation between the Tibetan winter snow and the Asian summer monsoon and rainfall: An observational investigation. *J. Climate*, **16**, 2038–2051.
- Yanai, M., C. Li, and Z. Song, 1992: Seasonal heating of the Tibetan Plateau and its effects on the evolution of the Asian summer monsoon. *J. Meteor. Soc. Japan*, **70**, 319–351.
- Ye, D., and Y. Gao, 1979: *The Meteorology of Qinghai–Xizang (Tibet) Plateau* (in Chinese). Science Press, 278 pp.
- Yu, R., B. Wang, and T. Zhou, 2004: Tropospheric cooling and summer monsoon weakening trend over East Asia. *Geophys. Res. Lett.*, **31**, L22212, doi:10.1029/2004GL021270.
- Zhang, Y., T. Li, and B. Wang, 2004: Decadal change of the spring snow depth over the Tibetan Plateau: The associated circulation and influence on the East Asian summer monsoon. *J. Climate*, **17**, 2780–2793.
- Zhao, P., Z. Zhou, and J. Liu, 2007: Variability of Tibetan spring snow and its associations with the hemispheric extratropical circulation and East Asian summer monsoon rainfall: An observational investigation. *J. Climate*, **20**, 3942–3955.
- Zhou, T., and R. Yu, 2005: Atmospheric water vapor transport associated with typical anomalous summer rainfall patterns in China. *J. Geophys. Res.*, **110**, D08104, doi:10.1029/2004JD005413.
- , D. Gong, J. Li, and B. Li, 2009: Detecting and understanding the multi-decadal variability of the East Asian summer monsoon—Recent progress and state of affairs. *Meteor. Z.*, **18**, 455–467.